



Cite this: *Chem. Commun.*, 2015, 51, 3566

Received 15th December 2014,  
Accepted 22nd January 2015

DOI: 10.1039/c4cc09988e

www.rsc.org/chemcomm

# Facile synthesis of magnetic homochiral metal–organic frameworks for “enantioselective fishing”†

Cui-Lan Chang,<sup>‡a</sup> Xiao-Yue Qi,<sup>‡a</sup> Jiang-Wei Zhang,<sup>b</sup> Ya-Ming Qiu,<sup>c</sup> Xian-Jiang Li,<sup>a</sup> Xin Wang,<sup>a</sup> Yu Bai,<sup>a</sup> Jun-Liang Sun<sup>c</sup> and Hu-Wei Liu<sup>\*a</sup>

**Magnetic functionalized homochiral metal–organic frameworks (MOFs) were prepared and applied to efficient enantioselective fishing of chiral drug intermediates. Under optimized conditions, the enantiomeric excess (ee) value as high as 85.2% was achieved for methyl phenyl sulfoxide (MPS) within 3 min.**

Chirality, referring to the property of the object or system not identical to its mirror image, has been confirmed to be closely related to the origin of life.<sup>1</sup> In chemistry, chirality is used to describe molecules that lack a symmetric plane. These chiral compounds, especially chiral drugs, often exhibit remarkably different effects in pharmacological activity, transport mechanisms, metabolism pathways and toxicity. So obtaining enantiomerically pure compounds is extremely important, and it is still a big challenge nowadays because of the identical physical and chemical properties of enantiomers in the achiral environment. Hence, development of new materials for chiral separation has been a hot area in chemical and pharmaceutical fields.<sup>2</sup>

Metal–organic frameworks (MOFs), known as a subclass of the coordination polymers, are crystalline materials generated by the association of metal ions and organic ligands.<sup>3</sup> They have emerged as a promising type of materials for their potential applications in gas storage,<sup>4</sup> separation<sup>5</sup> and catalysis<sup>6</sup> due to their fascinating structures. In latest studies, some homochiral MOFs have been used for enantioselective separation with good performance, indicating the promising application of homochiral

MOFs,<sup>7</sup> such as in direct enantioselective adsorption,<sup>8</sup> preparative chromatography,<sup>9</sup> gas chromatography,<sup>10</sup> liquid chromatography<sup>11</sup> and membrane separation.<sup>12</sup> Enantioseparation should be attributed to the interaction between the framework and racemic agents, such as hydrogen-bonding,<sup>8d,17a</sup> and the homochiral environment in the pores.<sup>17b</sup> Here, as an alternative approach, we pay attention to the magnetization of homochiral MOFs<sup>13</sup> and its application in enantioselective separation. Magnetic materials can be conveniently and fast separated from the medium by applying an external magnetic field.<sup>14</sup> In this work, for the first time, magnetic functionalized homochiral metal–organic frameworks (MOFs) were prepared by incorporation of magnetic iron oxide particles. These materials showed good performance in enantioselective separation of MPS with an ee value as high as  $\sim 85.2\%$ .

A homochiral MOF material,  $[\text{Zn}_2(\text{bdc})(\text{L-lac})(\text{dmf})](\text{DMF})$  (ZnBLD),<sup>15</sup> was selected for the preparation of magnetic homochiral MOFs *via* the reaction of  $\text{Zn}^{2+}$ , 1,4-benzenedicarboxylic acid and L-lactic acid. For preparing the magnetic homochiral MOFs, the incorporation of magnetic particles was a crucial factor.<sup>14b</sup> The reported ZnBLD was synthesized in Teflon-lined steel bombs under closed conditions without physical stirring, so it was difficult to form homogeneous composites of magnetic particles and homochiral MOFs by using this method.<sup>15</sup> To address this problem, we modified the synthesis approach of ZnBLD using a round-bottom flask in an oil-bath with magnetic stirring (see ESI† for details). Elemental analysis and powder X-ray diffraction (PXRD, Fig. S2 in ESI†) demonstrated that the coordination numbers and the skeleton structure were consistent with the reported homochiral MOFs synthesized in Teflon-lined steel bombs. Whereas, the properties of the channel changed due to the modified synthesis method. Single crystal X-ray data for ZnBLD:  $\text{C}_{36}\text{H}_{37}\text{NO}_{26}\text{Zn}_6$ ,  $M_r = 1291.89$ , orthorhombic,  $P2_12_12_1$ ,  $a = 8.0822(4)$ ,  $b = 20.8183(8)$ ,  $c = 30.8295(13)$  Å,  $V = 5187.3(4)$  Å<sup>3</sup>,  $Z = 4$ ,  $T = 293$  K,  $\rho_{\text{calcd}} = 1.417$  g cm<sup>−3</sup>,  $R_1 = 0.0443$ ,  $wR_2 = 0.1259$ ,  $\text{GoF} = 1.083$ ,  $\text{Flack} = 0.08(4)$ . CCDC-1033484 contains supplementary crystallographic data in detail.

As shown in Fig. S1 (ESI†), the coordination number of  $\text{Zn}^{2+}$  is five. It is worth noting that one of the coordinated oxygen

<sup>a</sup> Beijing National Laboratory for Molecular Sciences, Institute of Analytical Chemistry, College of Chemistry and Molecular Engineering, Peking University, Beijing, 100871, China. E-mail: hwlui@pku.edu.cn; Tel: +86-10-62754976

<sup>b</sup> Department of Chemistry, Tsinghua University, Beijing, 100084, China

<sup>c</sup> Beijing National Laboratory for Molecular Sciences, State Key Laboratory of Rare Earth Materials Chemistry and Applications, College of Chemistry and Molecular Engineering, Peking University, Beijing, 100871, China

† Electronic supplementary information (ESI) available: Experiment details, X-ray diffractogram, magnetization curve, TEM image, IR spectrum, recycle use and enantioselective ability. CCDC 1033484. For ESI and crystallographic data in CIF or other electronic format see DOI: 10.1039/c4cc09988e

‡ These authors contributed equally to this work.

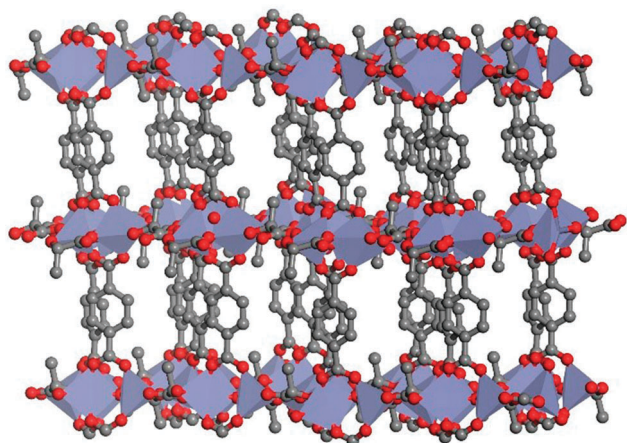


Fig. 1 3D framework of ZnBLD.

atoms comes from  $\text{H}_2\text{O}$  instead of DMF in this single crystal structure, which is different from the reported result.<sup>8c</sup> Chiral recognition functional pores formed by *L*-lactic ligands are interconnected and extend to three dimensional space (Fig. 1). Enantioselective separation could be achieved by homochiral MOFs because of the chiral-recognition environment formed by chiral ligands and open chiral channels or cavities.<sup>17</sup> The diameter of the pores is roughly 4 Å. As the molecular volume of  $\text{H}_2\text{O}$  is much smaller than that of DMF, the unit cell becomes smaller especially along the *a* axis, which is consistent with the fitting results of PXRD (Fig. S3 in ESI†). Overall, the homochiral environment is confined in a smaller space and effectively restrains nonspecific interaction, thus improving capture ability of chiral molecules. To some extent, the following experimental results exactly showed the improvement of the enantioselectivity.

Based on the successful synthesis of the ZnBLD using a round-bottom flask in an oil-bath with magnetic stirring, we further synthesized a magnetic functionalized homochiral ZnBLD ( $\text{Fe}_3\text{O}_4@\text{SiO}_2\text{-ZnBLD}$ ) (Fig. 2a). A certain amount of  $\text{Fe}_3\text{O}_4@\text{SiO}_2$  particles was added into the DMF solution of  $\text{Zn}(\text{NO}_3)_2$ , 1,4-benzenedicarboxylic acid and *L*-lactic acid. And then the resulting mixture was sonicated, stirred and heated at 120 °C for 24 h. The obtained solid was washed with DMF and ethanol before use. PXRD patterns of the  $\text{Fe}_3\text{O}_4@\text{SiO}_2\text{-ZnBLD}$ ,  $\text{Fe}_3\text{O}_4@\text{SiO}_2$  and ZnBLD are shown in Fig. 2b. Most of the diffraction peaks in PXRD patterns with  $2\theta$  from 5° to 40° for  $\text{Fe}_3\text{O}_4@\text{SiO}_2\text{-ZnBLD}$  composites were indexed to crystalline ZnBLD. The diffraction peaks in PXRD patterns with  $2\theta$  from 50° to 70° (shown in the black circle) correspond to  $\text{Fe}_3\text{O}_4@\text{SiO}_2$  in the composites. The intensity of  $\text{Fe}_3\text{O}_4@\text{SiO}_2$  was relatively low, which was due to the low contents of  $\text{Fe}_3\text{O}_4@\text{SiO}_2$  in the composites. At the same time, the IR spectrum (Fig. S6 in ESI†) of as-synthesized  $\text{Fe}_3\text{O}_4@\text{SiO}_2\text{-ZnBLD}$  composites contained the typical absorption features of  $\text{Fe}_3\text{O}_4@\text{SiO}_2$  and ZnBLD. In addition, the energy dispersive X-ray (EDX) analysis (Fig. 2c) of the composites also revealed the presence of Fe, Si and Zn. The corresponding morphology was identified by scanning electron microscopy (SEM, Fig. 2d) and transmission electron microscopy

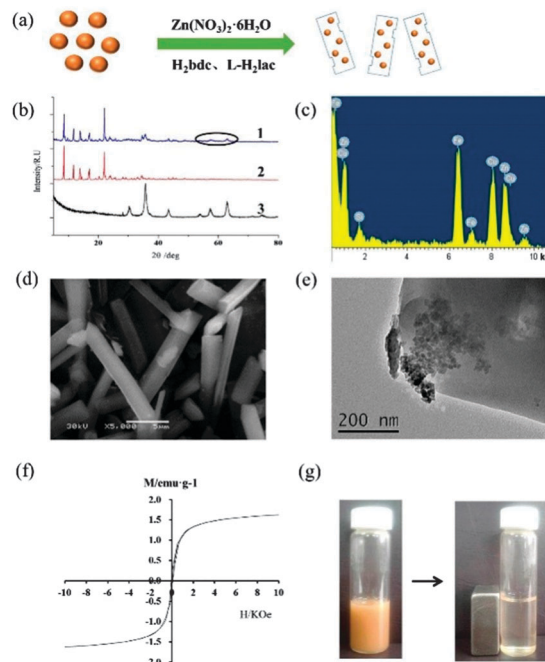


Fig. 2 Synthesis and characterization of  $\text{Fe}_3\text{O}_4@\text{SiO}_2\text{-ZnBLD}$  composites. (a) Schematic diagram of the synthesis approach; (b) PXRD patterns of  $\text{Fe}_3\text{O}_4@\text{SiO}_2\text{-ZnBLD}$  (1), ZnBLD (2) and  $\text{Fe}_3\text{O}_4@\text{SiO}_2$  (3); (c) EDS results of  $\text{Fe}_3\text{O}_4@\text{SiO}_2\text{-ZnBLD}$ ; (d) SEM image of  $\text{Fe}_3\text{O}_4@\text{SiO}_2\text{-ZnBLD}$ ; (e) TEM image of  $\text{Fe}_3\text{O}_4@\text{SiO}_2\text{-ZnBLD}$ ; (f) magnetization curve of  $\text{Fe}_3\text{O}_4@\text{SiO}_2\text{-ZnBLD}$ ; (g) separation of  $\text{Fe}_3\text{O}_4@\text{SiO}_2\text{-ZnBLD}$  from solution under an external magnetic field.

(TEM, Fig. 2e) techniques. The SEM image revealed that the  $\text{Fe}_3\text{O}_4@\text{SiO}_2\text{-ZnBLD}$  composites were mainly rod-like with a size range of 10–15  $\mu\text{m}$  and a diameter of  $\sim 1.5 \mu\text{m}$ . The TEM image demonstrated the presence of  $\text{Fe}_3\text{O}_4@\text{SiO}_2$  nanoparticles. Compared with the TEM image of  $\text{Fe}_3\text{O}_4@\text{SiO}_2$  (Fig. S5 in ESI†), although the distribution of  $\text{Fe}_3\text{O}_4@\text{SiO}_2$  in ZnBLD was not very homogeneous, the formed composites clearly showed the embedded structures with  $\text{Fe}_3\text{O}_4@\text{SiO}_2$  interspersed in ZnBLD. Besides, the magnetic measurements were conducted at room temperature to evaluate the magnetic behavior of the  $\text{Fe}_3\text{O}_4@\text{SiO}_2\text{-ZnBLD}$ . The saturated value of magnetization was measured to be 1.624  $\text{emu g}^{-1}$  (Fig. 2f), revealing strong magnetic properties. When a magnet was placed near the glass bottle with the dispersing solution of  $\text{Fe}_3\text{O}_4@\text{SiO}_2\text{-ZnBLD}$ , the magnetic particles were immediately attracted toward the magnet (Fig. 2g), which directly demonstrates the convenient separation of  $\text{Fe}_3\text{O}_4@\text{SiO}_2\text{-ZnBLD}$  composites from liquids by means of an external magnetic field.

MPS enantiomers can be used as both efficient synthetic auxiliaries and valuable pharmaceuticals, therefore, obtaining enantiomerically pure MPS is rather important.<sup>16</sup> Here,  $\text{Fe}_3\text{O}_4@\text{SiO}_2\text{-ZnBLD}$  composites were expected to select a single enantiomer from the racemic MPS solution and achieve the convenient separation of  $\text{Fe}_3\text{O}_4@\text{SiO}_2\text{-ZnBLD}$ -enantiomer complexes from the solution using an external magnet. This process can be vividly called “enantioselective fishing”, just as shown in Fig. 3a.  $\text{Fe}_3\text{O}_4@\text{SiO}_2\text{-ZnBLD}$  and racemic solution of

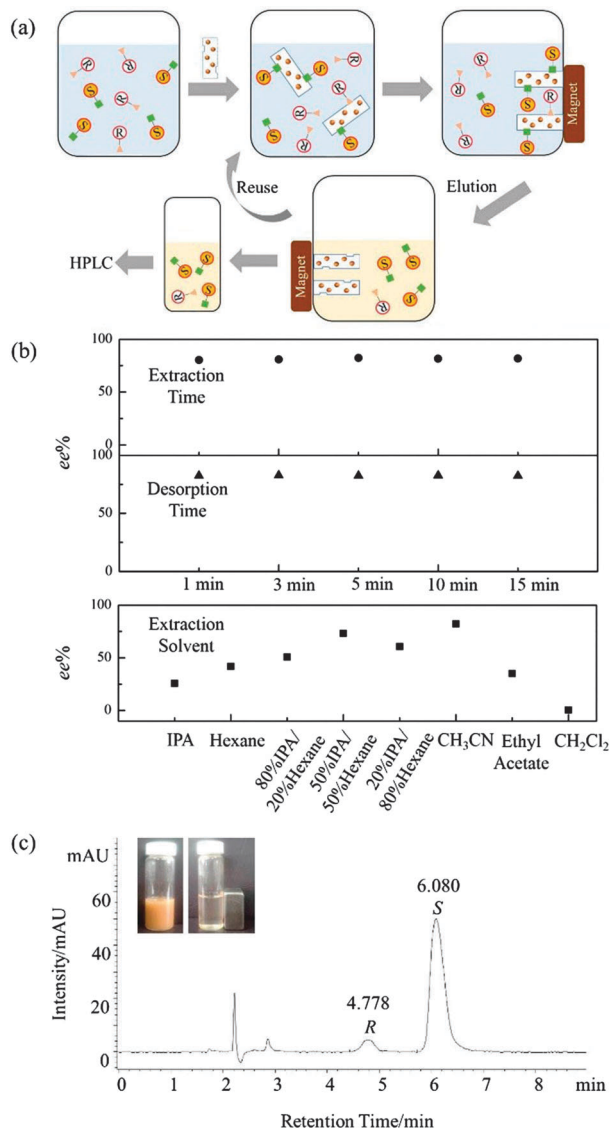


Fig. 3 "Enantioselective fishing" process performed using  $\text{Fe}_3\text{O}_4@\text{SiO}_2\text{-ZnBLD}$ . (a) Schematic diagram; (b) optimization of operation parameters; (c) optimized result for methyl phenyl sulfoxide.

MPS (final concentration is  $0.1 \text{ mg mL}^{-1}$ ) were added into a vial, shaken with a vortex mixer at room temperature and then the  $\text{Fe}_3\text{O}_4@\text{SiO}_2\text{-BLD}$ -enantiomer complexes were collected using a magnet. The collected  $\text{Fe}_3\text{O}_4@\text{SiO}_2\text{-ZnBLD}$ -enantiomer complexes were washed with methanol in order to retrieve the separated enantiomer and the enantiomeric composition of the separated enantiomer was analyzed by HPLC (Agilent Technology, USA) using a CHIRALCEL OD-3 column ( $4.6 \times 150 \text{ mm}$ ,  $3 \mu\text{m}$ , Daicel, Japan). Systematic optimization of the operation parameters was done to improve the enantioselective ability of  $\text{Fe}_3\text{O}_4@\text{SiO}_2\text{-ZnBLD}$ , including extraction solvent, extraction time and washing time (Fig. 3b). The results demonstrated that different extraction solvent had significant influence on the ee value. Among them, acetonitrile was much better than other solvents and gave the highest ee value. When the extraction time and washing time changed from 1 min to 15 min, the ee value

almost remained constant, which demonstrated the fast adsorption and desorption equilibrium between the  $\text{Fe}_3\text{O}_4@\text{SiO}_2\text{-ZnBLD}$  and the racemic solution of MPS. After the systematic optimization, acetonitrile was selected as the extraction solvent, and the extraction and washing time used was 1 min. Therefore, benefiting from the convenient and fast magnetic separation, the whole enantioselective adsorption process can be completed in no more than 3 min, which was much efficient than the conventional centrifugation and adsorption approach consuming more than 16 h.<sup>9,11c,15</sup> Additionally,  $\text{Fe}_3\text{O}_4@\text{SiO}_2\text{-ZnBLD}$  composites showed much higher preference for the (*S*)-enantiomer over the (*R*)-enantiomer due to the *L*-lactic acid in the homochiral MOF.<sup>9,15</sup> It is worth mentioning that the ee value was as high as 85.2%, which is much higher than the reported results of  $\sim 60\%$ .<sup>11c,14a,15</sup> And the adsorption amount of (*S*)-MPS could reach up to  $86.5 \mu\text{g mg}^{-1}$ . After being washed by methanol, the collected  $\text{Fe}_3\text{O}_4@\text{SiO}_2\text{-ZnBLD}$  can be reused at least six times with a high ee value of 80% (Fig. S7 in ESI†).

The enantioselective performance of this  $\text{Fe}_3\text{O}_4@\text{SiO}_2\text{-ZnBLD}$  was further studied using other sulfoxides including vinyl phenyl sulfoxide and 4-chlorophenyl methyl sulfoxide, and the results are shown in Table 1. Apparently, the corresponding ee values exhibited great difference among the three compounds due to the different substituents in molecules. Compared with MPS, the vinyl group in vinyl phenyl sulfoxide and  $-\text{Cl}$  in 4-chlorophenyl methyl sulfoxide had electron-withdrawing effect on the chiral center, which reduced the coordinating ability of the sulfoxides with  $\text{Fe}_3\text{O}_4@\text{SiO}_2\text{-ZnBLD}$ . Besides, the electron-withdrawing effect of  $-\text{Cl}$  in 4-chlorophenyl methyl sulfoxide was much larger than that of vinyl in vinyl phenyl sulfoxide. Hence, the ee value gradually decreased from MPS to 4-chlorophenyl methyl sulfoxide. In other words, MPS had the most appropriate coordination with  $\text{Fe}_3\text{O}_4@\text{SiO}_2\text{-ZnBLD}$  and showed higher ee value than other sulfoxides. These results are in good accordance with the previous report.<sup>9</sup>

As an alternative method, synthesis of another magnetic homochiral MOF, called  $\text{Fe}_3\text{O}_4@\text{SiO}_2\text{-ZnBDD}$ , was performed using *D*-lactic acid as the chiral ligand.  $\text{Fe}_3\text{O}_4@\text{SiO}_2\text{-ZnBDD}$  composites were expected to select another enantiomer from the racemic MPS solution. The operation parameters were the same as before. Each methanol solution was also analyzed by

Table 1 Enantioselective adsorption of model sulfoxides

Entry	Name	Structure	ee	
			$\text{Fe}_3\text{O}_4@\text{SiO}_2\text{-ZnBLD}$	$\text{Fe}_3\text{O}_4@\text{SiO}_2\text{-ZnBDD}$
1	Phenyl methyl sulfoxide		85.2% in <i>S</i> -enantiomer	86.2% in <i>R</i> -enantiomer
2	Phenyl vinyl sulfoxide		76.7% in <i>S</i> -enantiomer	77.0% in <i>R</i> -enantiomer
3	4-Chlorophenyl methyl sulfoxide		29.0% in <i>S</i> -enantiomer	29.9% in <i>R</i> -enantiomer

HPLC (Agilent Technology, USA) using the CHIRALCEL OD-3 column (4.6 × 150 mm, 3 μm, Daicel, Japan). The enantiomer separation results are summarized in Table 1. Fe<sub>3</sub>O<sub>4</sub>@SiO<sub>2</sub>-ZnBDD composites showed higher enantioselectivity for the (*R*)-enantiomer over the (*S*)-enantiomer due to the D-lactic acid in the homochiral MOF, and the ee value was as high as 86.2% (Fig. S8 in ESI†). Furthermore, the trends of the enantioselectivity with the variation of the groups in the three sulfoxides were consistent with those of Fe<sub>3</sub>O<sub>4</sub>@SiO<sub>2</sub>-ZnBLD composites. All of these results demonstrated that we can achieve convenient and efficient “enantioselective fishing” of MPS enantiomers using Fe<sub>3</sub>O<sub>4</sub>@SiO<sub>2</sub>-ZnBLD or Fe<sub>3</sub>O<sub>4</sub>@SiO<sub>2</sub>-ZnBDD composites.

In conclusion, we have demonstrated that Fe<sub>3</sub>O<sub>4</sub>@SiO<sub>2</sub> tagged to an appropriate homochiral ZnBLD or ZnBDD can be utilized for “enantioselective fishing” of enantiomers in magnetic field. Benefitting from the magnetic separation, the whole process can be completed in 3 min. Fe<sub>3</sub>O<sub>4</sub>@SiO<sub>2</sub>-ZnBLD and Fe<sub>3</sub>O<sub>4</sub>@SiO<sub>2</sub>-ZnBDD composites showed much higher preference for the (*S*)-enantiomer or (*R*)-enantiomer with an ee value of 85.2% and 86.2%, respectively. After being reused six times, the enantioselective ability remained almost constant and demonstrated the stability of these composites. Even though the complete separation of the two enantiomers was not achieved in this study, the convenience and efficiency of Fe<sub>3</sub>O<sub>4</sub>@SiO<sub>2</sub>-ZnBLD and Fe<sub>3</sub>O<sub>4</sub>@SiO<sub>2</sub>-ZnBDD will make this approach promising in the enantiomer separation in the future.

This work was financially supported by the National Natural Science Foundation of China (Grant No. 21027012 and 21275012).

## Notes and references

- (a) T. L. V. Ulbricht, *Nature*, 1975, **258**, 383–384; (b) J. B. Youatt and R. D. Brown, *Science*, 1981, **212**, 1145–1146.
- (a) C. L. Chang, X. Wang, Y. Bai and H. W. Liu, *TrAC, Trends Anal. Chem.*, 2012, **39**, 195–206; (b) T. J. Ward and K. D. Ward, *Anal. Chem.*, 2012, **84**, 626–635.
- (a) O. M. Yaghi and Q. W. Li, *MRS Bull.*, 2009, **34**, 682–690; (b) S. Kitagawa, R. Kitaura and S. Noro, *Angew. Chem., Int. Ed.*, 2004, **43**, 2334–2375; (c) H. Furukawa, K. E. Cordova, M. O’Keeffe and O. M. Yaghi, *Science*, 2013, **341**, 974–986.
- (a) S. S. Kaye, A. Dailly, O. M. Yaghi and J. R. Long, *J. Am. Chem. Soc.*, 2007, **129**, 14176–14177; (b) J. G. Vitillo, L. Regli, S. Chavan, G. Ricchiardi, G. Spoto, P. D. C. Dietzel, S. Bordiga and A. Zecchina, *J. Am. Chem. Soc.*, 2008, **130**, 8386–8396.
- (a) U. Mueller, M. Schubert, F. Teich, H. Puetter, K. Schierle-Arndt and J. Pastre, *J. Mater. Chem.*, 2006, **16**, 626–636; (b) M. R. Lohe, K. Gedrich, T. Freudenberger, E. Kockrick, T. Dellmann and S. Kaskel, *Chem. Commun.*, 2011, **47**, 3075–3077.
- (a) G. Nickerl, A. Henschel, R. Grunker, K. Gedrich and S. Kaskel, *Chem. Ing. Tech.*, 2011, **83**, 90–103; (b) M. Yoon, R. Srirambalaji and K. Kim, *Chem. Rev.*, 2012, **112**, 1196–1231; (c) J. Park, J. R. Li, Y. P. Chen, J. M. Yu, A. A. Yakovenko, Z. Y. U. Wang, L. B. Sun, P. B. Balbuena and H. C. Zhou, *Chem. Commun.*, 2012, **48**, 9995–9997; (d) F. J. Song, C. Wang and W. B. Lin, *Chem. Commun.*, 2011, **47**, 8256–8258; (e) K. Leus, Y.-Y. Liu and P. Van Der Voort, *Catal. Rev.: Sci. Eng.*, 2014, **56**, 1–56.
- X. J. Li, C. L. Chang, X. Wang, Y. Bai and H. W. Liu, *Electrophoresis*, 2014, **35**, 2733–2743.
- (a) G. Li, W. B. Yu and Y. Cui, *J. Am. Chem. Soc.*, 2008, **130**, 4582–4583; (b) Y. Liu, W. M. Xuan and Y. Cui, *Adv. Mater.*, 2010, **22**, 4112–4135; (c) R. Vaidhyanathan, D. Bradshaw, J. N. Rebilly, J. P. Barrio, J. A. Gould, N. G. Berry and M. J. Rosseinsky, *Angew. Chem., Int. Ed.*, 2006, **45**, 6495–6499; (d) R. Bueno-Perez, A. Martin-Calvo, P. Gomez-Alvarez, J. J. Gutierrez-Sevillano, P. J. Merklings, T. J. Vlugt, T. S. van Erp, D. Dubbeldam and S. Calero, *Chem. Commun.*, 2014, **50**, 10849–10852.
- A. L. Nuzhdin, D. N. Dybtsev, K. P. Bryliakov, E. P. Talsi and V. P. Fedin, *J. Am. Chem. Soc.*, 2007, **129**, 12958–12959.
- (a) S. M. Xie, Z. J. Zhang, Z. Y. Wang and L. M. Yuan, *J. Am. Chem. Soc.*, 2011, **133**, 11892–11895; (b) J. Dong, Y. Liu and Y. Cui, *Chem. Commun.*, 2014, **50**, 14949–14952; (c) Y. Peng, T. Gong and Y. Cui, *Chem. Commun.*, 2013, **49**, 8253–8255.
- (a) X. Kuang, Y. Ma, H. Su, J. Zhang, Y. B. Dong and B. Tang, *Anal. Chem.*, 2014, **86**, 1277–1281; (b) M. Padmanaban, P. Muller, C. Lieder, K. Gedrich, R. Grunker, V. Bon, I. Senkovska, S. Baumgartner, S. Opelt, S. Paasch, E. Brunner, F. Glorius, E. Klemm and S. Kaskel, *Chem. Commun.*, 2011, **47**, 12089–12091; (c) K. Tanaka, T. Muraoka, D. Hirayama and A. Ohnishi, *Chem. Commun.*, 2012, **48**, 8577–8579; (d) M. Zhang, Z. J. Pu, X. L. Chen, X. L. Gong, A. X. Zhu and L. M. Yuan, *Chem. Commun.*, 2013, **49**, 5201–5203.
- (a) W. J. Wang, X. L. Dong, J. P. Nan, W. Q. Jin, Z. Q. Hu, Y. F. Chen and J. W. Jiang, *Chem. Commun.*, 2012, **48**, 7022–7024; (b) Z. Kang, M. Xue, L. Fan, J. Ding, L. Guo, L. Gao and S. Qiu, *Chem. Commun.*, 2013, **49**, 10569–10571; (c) K. Huang, X. Dong, R. Ren and W. Jin, *AIChE J.*, 2013, **59**, 4364–4372.
- R. Ricco, L. Malfatti, M. Takahashi, A. J. Hill and P. Falcaro, *J. Mater. Chem. A*, 2013, **1**, 13033–13045.
- (a) H. J. Choi and M. H. Hyun, *Chem. Commun.*, 2009, 6454–6456; (b) F. Ke, Y. P. Yuan, L. G. Qiu, Y. H. Shen, A. J. Xie, J. F. Zhu, X. Y. Tian and L. D. Zhang, *J. Mater. Chem.*, 2011, **21**, 3843–3848.
- D. N. Dybtsev, A. L. Nuzhdin, H. Chun, K. P. Bryliakov, E. P. Talsi, V. P. Fedin and K. Kim, *Angew. Chem., Int. Ed.*, 2006, **45**, 916–920.
- I. Fernandez and N. Khiar, *Chem. Rev.*, 2003, **103**, 3651–3705.
- (a) Z.-X. Xu, Y.-X. Tan, H.-R. Fu, Y. Kang and J. Zhang, *Chem. Commun.*, 2014, DOI: 10.1039/C4CC09821H; (b) H.-X. Zhang, F. Wang, Y.-X. Tan, Y. Kang and J. Zhang, *J. Mater. Chem.*, 2012, **22**, 16288–16292; (c) S. Qiu, M. Xue and G. Zhu, *Chem. Soc. Rev.*, 2014, **43**, 6116–6140.